Josephson effect and Andreev reflection
in $Ba_{1−x}Na_xFe_2As_2$ (x = 0.25 and 0.35) point contacts

V.V. Fisun[1], O.P. Balkashin[1], O.E. Kvitnitskaya[1], I.A. Korovkin[1],
N.V. Gamayunova[1], S. Aswartham[2], S. Wurmehl[2], and Yu.G. Naidyuk[1]

[1]*B. Verkin Institute for Low Temperature Physics and Engineering National Academy of Sciences of Ukraine*
47 Lenin Ave., Kharkov 61103, Ukraine
E-mail: naidyuk@ilt.kharkov.ua

[2]*Leibniz-Institut für Festkörper- und Werkstoffforschung Dresden e.V.,*
Postfach 270116, Dresden D-01171, Germany

$I(V)$ characteristics and their first derivatives of ScS and ScN-type (S is superconductor, c is constriction, N is normal metal) point contacts (PCs) based on $Ba_{1−x}Na_xFe_2As_2$ (x = 0.25 and 0.35) were studied. ScS-type PCs with S = Nb,Ta, and Pb show Josephson-like resistively shunted $I(V)$ curves with microwave induced Shapiro steps which satisfy relation $2eV = \hbar\omega$. The I_cR_N product (I_c is critical current, R_N is normal state PC resistance) in these PCs is found to be up to 1.2 mV. All this data with the observed dependence of the I_c on the microwave power of ScS PCs with Pb counterelectrode indicates the presence of the singlet s-wave type pairing in $Ba_{1−x}Na_xFe_2As_2$. From the $dV/dI(V)$ curves of ScN-type PCs demonstrating Andreev-reflection like features, the superconducting gap Δ ratio $2\Delta/k_BT_c = 3.6 \pm 1$ for the compound with x = 0.35 was evaluated. Analysis of these $dV/dI(V)$ at high biases V, that is well above Δ, testifies transition to the thermal regime in PCs with a voltage increase.

PACS: **74.50.+r** Tunneling phenomena; Josephson effects;
74.70.Dd Ternary, quaternary, and multinary compounds;
74.45.+c Proximity effects; Andreev reflection; SN and SNS junctions.

Keywords: point contacts, Josephson effects, Shapiro steps, Andreev reflection.

1. Introduction

The discovery of superconductivity in the iron-based materials provokes an enormous interest, since a high T_c was obtained in compounds with ferromagnetic metals, what raised the question about nature of superconducting (SC) pairing mechanism and symmetry of SC wave function. Ferriferous doped superconductors of 122-type structure based on the parent compound $BaFe_2As_2$ are the most investigated pnictide systems nowadays. Hole doping by alkali metals leads to the suppression of the spin-density wave antiferromagnetic state and the appearance of superconductivity with transition temperature T_c up to 38 K [1,2]. Superconductivity is formed here in a multiband system with multiple Fermi surfaces of different (electron and hole) nature, which is very different from the single band situation in high-T_c cuprates. Since their discovery, quite a lot of research has been done, in which the electron spectrum and the Fermi surface of new superconductors were studied using angle-resolved photoemission (ARPES) [3]. This meth-od has proved its effectiveness in the physics of high-T_c cuprates. In fact, for iron-based superconductors ARPES-study provides valuable information that helps clarify the peculiarities of their electronic spectrum, as well as of the Fermi surface, and the quantities and characteristics of SC gap(s). Investigation of the Josephson effect [4] and point-contact Andreev-reflection (PCAR) spectroscopy [5] plays significant role in the understanding of the nature of the SC ground state in these material as well.

The Josephson effect [6,7] was investigated in pressure-type contacts with the Pb counterelectrode in [8]. Stable Josephson coupling in contacts $Ba_{1−x}Na_xFe_2As_2$–Pb along the c-axis was found. It was established that a Josephson current flows mainly through the active small contacts which exhibit virtually no superconductivity at low clamping. Just as the pressure increases, the contact area increases and superconductivity appears. Observation of the Josephson effect in the c-axis geometry in this iron pnictides excludes pure p- or d-wave pairing in these materials and

the obtained results support the existence of *s*-wave pairing [9]. Josephson junctions fabricated in epitaxial films utilizing bicrystal grain boundary [10] and oxidized titanium layers as barriers [11] have been studied as well. Both studies report also some difficulty to get junctions with Josephson behavior and the product $I_c R_N$ is up to several orders of magnitude less than that expected theoretically, what is a serious obstacle for an application.

On the other hand, PCAR spectroscopy is widely used to study SC order parameter(s) or SC gap(s) in these compounds [5,12,13]. In our paper [14] we utilized the PCAR spectroscopy to study the SC gap in the sample with $x =$ $= 0.25$. It was shown that pronounced peculiarities in the PC spectra at high biases above the SC gap is governed by high specific resistivity and thermopower of the bulk material being the features of the thermal regime of the current flow in PCs. Whereas emerging of Andreev reflection (AR) structures at small biases gave possibility for the spectroscopy of the SC gap which showed unequivocally only one gap with the preferred value $2\Delta/k_B T_c \approx 6$. In this study we continue PCAR investigation of the $Ba_{1-x}Na_x Fe_2 As_2$ family, focusing on the compound with $x = 0.35$, in order to have a look on the gap structure in this compound and compare with the results obtained in [14] for $x = 0.25$.

2. Experimental details

Single crystals of $Ba_{1-x}Na_x Fe_2 As_2$ were grown using a self-flux high-temperature solution growth technique [15]. For the samples with $x = 0.25$ and 0.35 the SC transition in resistivity starts around 10 and 34 K, correspondingly.

The PCs were established *in situ* by touching a thin metallic wire ($\varnothing \approx 0.2$–0.3 mm) to the cleaved (at room temperature) surface (an edge) of the plate-like (flake) sample. Thus, we measured heterocontacts between simple metal and the title compound preferably in the *ab*-plane. The differential resistance $dV/dI(V) \equiv R(V)$ of $I(V)$ characteristic of PC was recorded by sweeping the dc current I on which a small ac current i was superimposed using standard lock-in technique. The measurements were performed mainly at the temperature 4.2 K (up to 35 K in some cases) and under microwave irradiation with frequency 9.57 GHz in the case of ScS contacts.

The critical current I_c (Josephson effect) was registered on $I(V)$ curves of ScS contacts only after electrical breakdown of mechanically established PC from resistance of a few tenth Ohm till much lower resistance, i.e., much less than 1 Ω. For PCs with Pb counterelectrode we were able to produce Josephson junctions with a clear critical current or zero resistance at $V = 0$, while in the case of the Ta and Nb counterelectrodes an additional resistance appeared, so that $R(V = 0) \neq 0$.

The characteristic voltage $V = I_c R_N$ (R_N is normal state resistance of PC) that determines the cutoff frequency of the Josephson current [16], was up to $V = 1.2$ meV for

the PCs with Pb counterelectrode. Induced Shapiro steps were observed under microwave irradiation both on $I(V)$ curves and more clearly on their first derivatives with the distance between them $V = \hbar\omega/2e$.

For some ScS contacts with the Pb counterelectrode, as well as for all contacts with the Ta counterelectrode, the critical current was very small and the manifestation of the ac Josephson effect (Shapiro steps) was observed only on the first derivatives of the $I(V)$. Equivalent circuit for PCs in this case, can be represented as a series connection of the resistance with a Josephson junction. In the case of Nb counterelectrode a more complex circuit was implemented with serial and parallel additional resistances as it will be shown further.

3. Results and discussion

3.1. Search for Josephson effect in ScS contacts

Figure 1 shows a series of the $I(V)$ curves and first derivative of a ScS PC $Ba_{1-x}Na_x Fe_2 As_2$ with Pb counterelectrode at different microwave power levels. It is noticeable that under irradiation stepped structure occurs in the $I(V)$. This is, so-called, Shapiro steps, or manifestation of the *ac* Josephson effect [6,7].

For some contacts with the Pb counterelectrode (Fig. 2) there was a significant slope of $I(V)$ at $V = 0$ and the critical current was small. This leads to the fact that the distance between the steps becomes larger than the expected one. The $I(V)$ slope at $V = 0$ indicates the inclusion of an additional resistance R_{ad} in series with the Josephson junction (see the equivalent circuit in Fig. 2). Accounting of this resistance ($R_{ad} = 28$ mΩ) leads to the elimination of $I(V)$ inclination at $V = 0$ (Fig. 2 inset), while appropriate distance between steps Shapiro becomes $V = \hbar\omega/2e$ as it should be in the case of Josephson coupling. It should be noted that the induced current steps with the largest num-
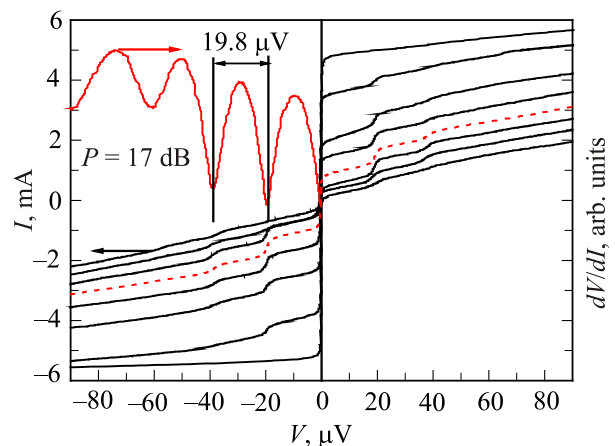

Fig. 1. (Color online) $I(V)$ curves of contact $Ba_{1-x}Na_x Fe_2 As_2$ – Pb at increasing of microwave power from zero (top curve) to the maximal (bottom curve). For the dotted (red) $I(V)$ curve its first derivative dV/dI is shown for negative bias. $T = 4.2$ K, $f = 9.57$ GHz.
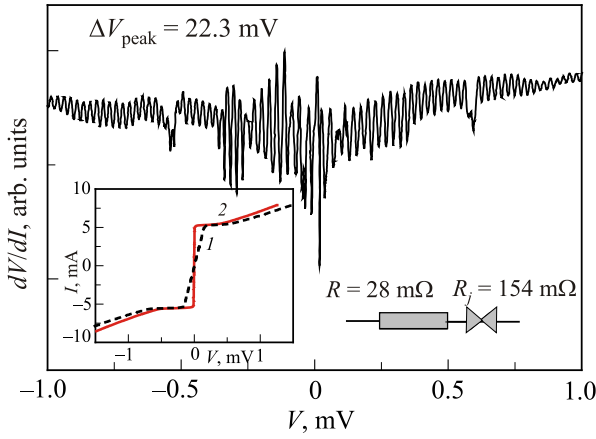
Fig. 2. (Color online) First derivative of $I(V)$ curve of $Ba_{1-x}Na_xFe_2As_2$ – Pb contact. Inset: experimental $I(V)$ (dotted curve *1*), solid curve *2* is $I(V)$ after subtracting of additional resistance.

ber was observed at $V \sim 1$ mV. This value coincides with the characteristic voltage estimated from the product of I_cR_N.

The position of current steps on the voltage axis is defined by the Josephson relation [6,7]:

$$V_n = nhf/2e, \quad n = 0, 1, 2, 3,... \quad (1)$$

with a superconducting pair charge equal to $2e$. It is known [6,7] that the height of the current steps induced by the external field oscillates with increase of the irradiation power. The amplitude of the current steps is given by the Bessel function of the corresponding order [6,7]:

$$I_n = I_0 \, | J_n(e\nu/hf) |, \quad (2)$$

where $\nu \sim \sqrt{P}$ (P is microwave power) is ac voltage induced in a contact by microwave field. Figure 3 shows dependence of the critical current I_c and the first two steps of currents I_1 and I_2 on the microwave power. The resulting curves are in good agreement with the initial portions of the corresponding Bessel functions [7]. Since the investigated Josephson junctions have low resistance ($R_N < 0.2 \, \Omega$) then we do not have enough microwave power to trace the behavior of the critical current I_c and the first two steps of the currents I_1 and I_2 to a greater extent.

In the case of the Ta counterelectrode, electrical breakdown is also used to create a Josephson junction. However, in this case, there was always a significant slope of $I(V)$ at $V = 0$ and thus the critical current was negligible. This leads to the observation that Shapiro steps become visible only on the first derivative $dV/dI(V)$ as dips and the distance between them was greater than the expected one (Fig. 4). Thus, for the ScS contacts with the Ta counterelectrode the equivalent circuit includes a series resistance, as well as for some PCs with Pb. Accounting for this resistance $R_{ad} = 21.7$ mΩ leads to the elimination of
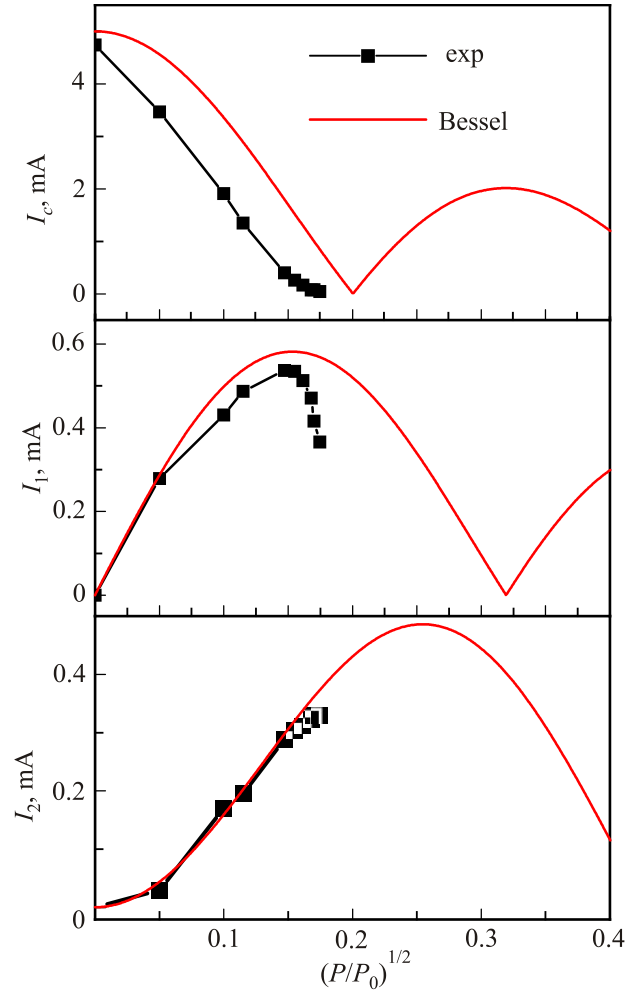

Fig. 3. (Color online) Dependence of the critical current I_c and the amplitude of the first microwave induced steps of a currents I_1 and I_2 on microwave power P.

$I(V)$ inclination at $V = 0$ and the distance between Shapiro steps becomes correct, i.e., $V = \hbar\omega/2e$.

Josephson junctions with a counter electrode made of Nb, as well as in the case of Ta and Pb, had also a slope of $I(V)$ at $V = 0$ and a larger distance between Shapiro steps. The equivalent circuit here is more complicated, since the incorporation of additional resistance in the circuit with series connection leads to overestimation of distance between the steps. The equivalent circuit of a ScS contact in this case, following [17], can be represented as a parallel circuit, in one arm, which includes a Josephson junction in series with the resistance R_1, and the other — an additional parallel resistance R_2. It is assumed that the resistive elements have a linear $I(V)$ and the power of the incident radiation is sufficiently low to prevent bolometric effect, i.e., the contact heating by irradiation is negligible.

Applying the methodology outlined in [17] to our ScS contacts with Ta and Nb, we show the final electrical circuits in Fig. 4 (insets).
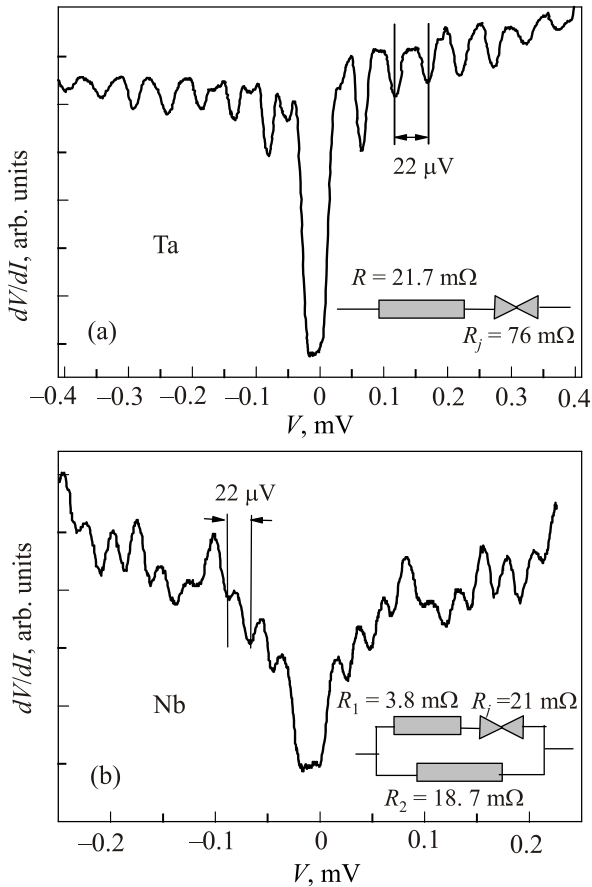
Fig. 4. (Color online) The first derivative of $I(V)$ for a ScS contact Ba$_{1-x}$Na$_x$Fe$_2$As$_2$ – Ta at $T = 4.2$ K, $f = 9.57$ GHz. Shapiro steps appear as dips spaced by 22 μV. The inset shows the equivalent circuit of a Josephson junction with serial resistance accounting for additional resistance (a). The first derivative of $I(V)$ for a ScS contact Ba$_{1-x}$Na$_x$Fe$_2$As$_2$ – Nb at $T = 4.2$ K, $f = = 9.57$ GHz. Shapiro steps appear as dips spaced by 23 μV. The insets shows the equivalent circuit of a Josephson junction with the additional serial and parallel resistances (b).

The absence of the critical current (nonzero resistance at $V = 0$) on $I(V)$ in the case of the Ta and Nb counterelectrodes makes it impossible to trace its behavior as a function of the microwave power. Difficulties associated with the creation of Josephson junctions with high critical parameters in the case of Ta and Nb counterelectrodes, can be connected with sensitivity of the SC parameters of pnictides to stoichiometry of the surface. It may be associated with degradation of the surface structure of Ba$_{1-x}$Na$_x$Fe$_2$As$_2$ in the contact. Namely, Pb is a softer counterelectrode compared with Ta and Nb, what reduces the surface damage at the PC creating.

Thus, the detection of the ac Josephson effect in point contacts between Ba$_{1-x}$Na$_x$Fe$_2$As$_2$ crystals and Pb, Ta, and Nb counterelectrode with the distance between Shapiro steps $V = \hbar\omega/2e$, as well as the observed dependence of the critical current on the microwave power with Pb

counterelectrode is in line with the presence of the singlet s-wave pairing in this new superconductor.

3.2. Andreev reflection spectroscopy using ScN contacts

We have measured and analyzed a few tens of $dV/dI(V)$ dependences of Ba$_{1-x}$Na$_x$Fe$_2$As$_2$–Ag (or Cu) ScN-type PCs. As in the case of the samples with $x = 0.25$ [14], the $dV/dI(V)$ spectra do not show any principal difference while being measured by attaching the needle to the cleaved surface or to an edge of the samples. While measuring different PCs below transition temperature T_c the various shapes of dV/dI were observed. They are shown in Fig. 5 for several PCs. Let us consider peculiarities of $dV/dI(V)$ in Fig. 5. Some of them are supposed to be due to Andreev reflection effect. These are the double dV/dI minima at energies roughly corresponding to the SC energy gap. These features are visible in two upper dV/dI characteristics shown in Fig. 5. The position of the dV/dI minima appear to be in the range between 5 and 15 meV for different PCs. Whereas two lower PCs in Fig. 5 are presumably in the thermal limit of the current flow and their dV/dI shape is caused by the bulk resistivity and thermal effects as mentioned in [14] for compound with $x = 0.25$. The middle curve shows the shallow AR-like minima around $V = 0$ followed by spikes, while its further behavior is similar to that of two bottom curves at large bias. That is this spectrum looks like transitional one between the upper and the lower spectra. The much larger change of the differential resistance for two lower dV/dI also confirms the realization of the thermal regime for these PCs. We should also mention that unlike the system with $x = 0.25$ investigated earlier [14], where the local T_c in PCs had a large dispersion, i.e., from 10 K up to 20 K and higher, the actual samples showed a rather stable local T_c being around 30 K. Also the dV/dI curves of the samples with $x = 0.35$ did not display a pronounced Kondo-like shape above T_c as some of those of the specimen with $x = 0.25$. All this points to a better homogeneity and quality of the investigated samples with $x = 0.35$ at least on the surface.

The necessary condition for receiving of the spectroscopic information from the PC data (among them is the SC gap) is the fulfilment of the spectroscopic (nonthermal) regime of the current flow through PC [18]. In this case the size (diameter d) of PCs should be less than inelastic mean free path l_i of electrons and an additional requirement $d < \xi$ for PCs (ξ is the coherence length) is desirable to prevent the variation of the order parameter (SC gap) in the PC core. As we mentioned in [14], the elastic electronic mean-free path in Ba$_{1-x}$Na$_x$Fe$_2$As$_2$ is small (to be about 10 nm) and the coherence length ξ amounts to only 2 nm in the isostructural system Ba$_{1-x}$K$_x$Fe$_2$As$_2$ [19]. Evaluation of the typical PC diameter for investigated PCs, as made in [14], gives for the PC size values between 2 and 200 nm for the PC resistances from 1 to 110 Ω. Thus, only for very high-ohmic PCs the ballistic (spectroscopic) re-

gime can be realized. Therefore, we suppose the possibility of the diffusive regime for low-ohmic PCs at small voltage biases. Another criterion of the spectral regime is the observation of AR-like features in the *dV/dI(V)* curves in the SC state.

One of the main tasks at the interpretation of PC data in systems with very short electronic lengths is the separation of the "thermal" features from the spectral ones. It is commonly known that in the thermal regime $l_i \ll d$ the temperature inside PC increases with the bias voltage according to the Kohlrausch relation [18,20]:

$$T_{PC}^2 = T_{bath}^2 + V^2/4L_0, \qquad (3)$$

where T_{PC} is the temperature in the PC core, T_{bath} is the temperature of the bath and L_0 is the Lorentz number ($L_0 = 2.45 \cdot 10^{-8}$ V^2/K^2). In this case, the shape of *I(V)* characteristic for PC is determined by the bulk resistivity $\rho(T)$ according to Kulik's thermal model [20,21] as:

$$I(V) = Vd \int_0^1 \frac{dx}{\rho(T_{PC}\sqrt{1-x^2})}. \qquad (4)$$

First, we have calculated *dV/dI(V)* according to Eq. (4) for several PCs in the thermal regime within this model using the temperature dependence of the bulk resistivity $\rho(T)$ from [15] for the investigated system. The obtained result for one of PC (left inset in Fig. 6) demonstrates the good qualitative and quantitative correlation with experimental data in the bias region above the SC peculiarities. This proves the realization of the thermal regime. For this calculation we used the following parameters: the residual resistivity $\rho_0^{PC} \approx 80$ μΩ·cm, $d = 140$ nm, $L = 2.8 L_0$. Note, that the Lorentz number L is larger than the standard value. An enhanced L may be due to the additional contribution of phonons to the thermal conductivity of PC through electrically nonconductive osculant surfaces.

We should note that measured *dV/dI(V)* characteristics of the investigated compound are asymmetric having larger *dV/dI(V)* values for the positive bias. The similar asymmetry was also reported in [14] for the samples with $x = 0.25$. In Fig. 6, we present the antisymmetric part of *dV/dI(V)*^{a} ≡ ≡ $R^a(V)$ for the PC from Fig. 5. The calculated $R^a(V)$ demonstrates a broad maximum at about 70–80 mV. Qualitatively, the shape of the latter corresponds well to the temperature dependence of the thermopower $S(T)$ measured for the isostructural compound Ba$_{0.7}$K$_{0.3}$Fe$_2$As$_2$ [22] (see right inset in Fig. 6). This fact points out to that the PCs at high bias are certainly in the thermal regime while at the low bias the spectral regime is possible. Detail analysis of the thermal regime is given in [14] for the sample with $x = 0.25$.

Let's turn to *dV/dI(V)* curves with AR-like shape shown on Fig. 5. Figure 7 presents the temperature measurements of
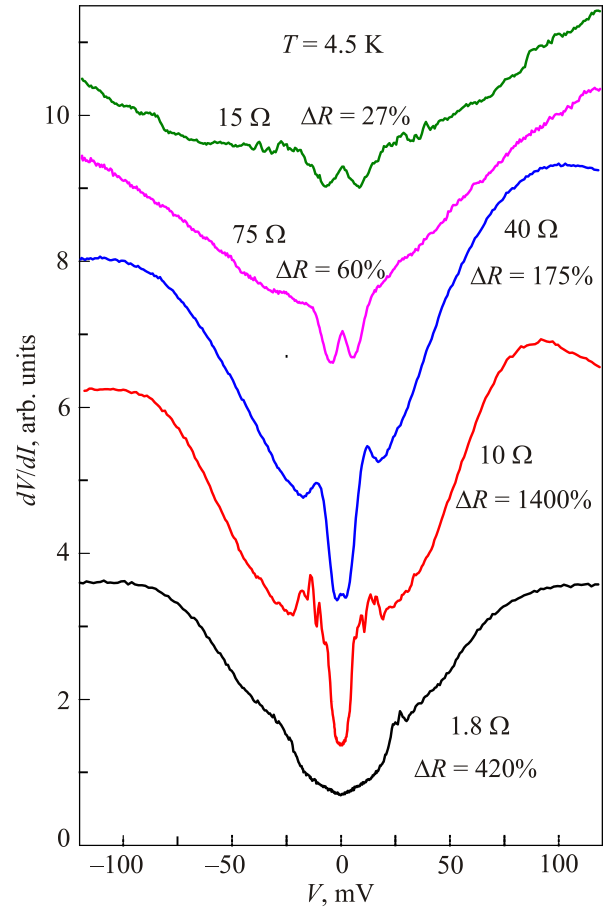

Fig. 5. (Color online) *dV/dI(V)* curves displaying the SC features (deep minima) around zero-bias for the PCs with different resistance R (R is measured just above the SC minimum at $V > \Delta/e$)). The change $\Delta R = (R(V = 100$ mV$) - R(V = 0))/R(V = 0)$ of the PC resistance is shown in per cents for each PC. The curves are shifted for the clarity.

the *dV/dI(V)* in a wide temperature range. Two curves measured at lowest and highest temperature in a wide voltage range are shown separately in the inset. Like in the case of compounds with $x = 0.25$ [14], the *dV/dI(V)* curves possess a pronounced asymmetry and display high-bias maxima (here at about ± 100 mV). Besides, at the lowest temperatures *dV/dI(V)* displays zero-bias minima, which are likely due to Andreev reflection. At the temperature rise they transform to a single minimum with the decrease of its amplitude. Finally it vanishes above 25 K, what is close to T_c of the bulk sample for $x = 0.35$. Calculation of the SC gap using conventional BTK fit procedure [5] results in $\Delta \simeq 3.7$ meV for this PC and the reduced gap value $2\Delta/k_B T_c \simeq 2.8$–3.4 if we take T_c in the range 25–30 K, where the dip minimum in *dV/dI* on in Fig. 7 disappears. Remind, that above we paid attention that this PC may be affected by heating with voltage increase and the developed peaks around ± 10 mV may influence the gap determination.

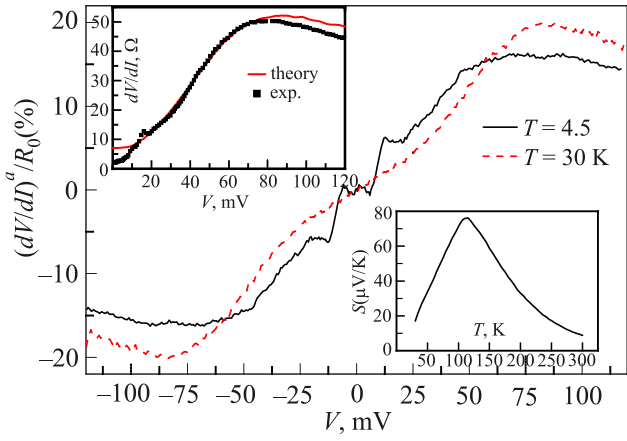**Fig. 6.** (Color online) Calculated antisymmetric part $dV/dI(V)^a =$ $= 100 R(V > 0) - R(V < 0))/2R(V = 0)$ of PC from Fig. 5 with $R =$ 40 Ω at two different temperatures 4.5 and 30 K. Right inset: Temperature dependence of the thermopower S in $Ba_{0.7}K_{0.3}Fe_2As_2$ [22]. Left inset: Symmetrized $dV/dI(V)$ for the PC with $R = 1.8$ Ω (points) from Fig. 5 measured at $T = 4.5$ K along with the calculated $dV/dI(V)$ according to Eq. (4) (solid line). To fit the position of the maxima we used an enhanced Lorenz number $L = 2.8L_0$ in the calculation.

So, we have carried out similar procedure (fit) for a PC ($R_N \simeq 75$ Ω) from Fig. 5 with more pronounced AR minima. The results are shown in Fig. 8. For this PC $\Delta \simeq 6$ meV is larger and the reduced gap value $2\Delta/k_B T_c \simeq 4.7$, where T_c is taken from the BCS curve in Fig. 8, because this PC has not survived the temperature increase above 20 K. The reduced gap value estimated from the BTK fit using the local T_c in other PCs results in average to $2\Delta/k_B T_c = 3.6 \pm 1$. As we mentioned above for the compound with $x = 0.25$ the larger value $2\Delta/k_B T_c \approx 6$ was found. So, the difference be-
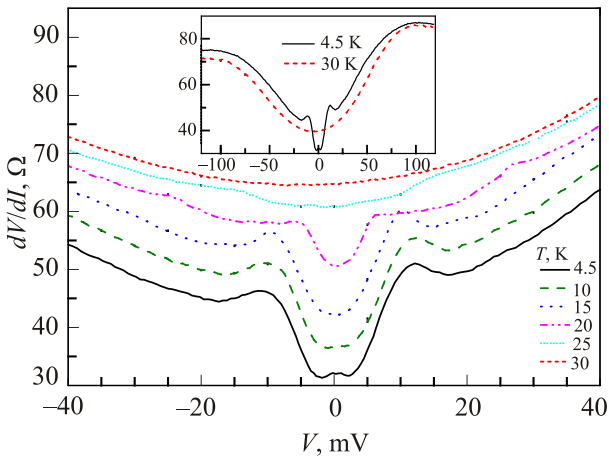

Fig. 7. (Color online) $dV/dI(V)$ curves measured for the $Ba_{0.65}K_{0.3}Fe_2As_2$ –Cu PC from Fig. 5 with $R \approx 40$ Ω at various temperatures. The curves, except the bottom one, are shifted for better vizualization. Inset: dV/dI of this PC recorded in a wider bias range for the lowest (4.5 K) and highest (30 K) temperature.
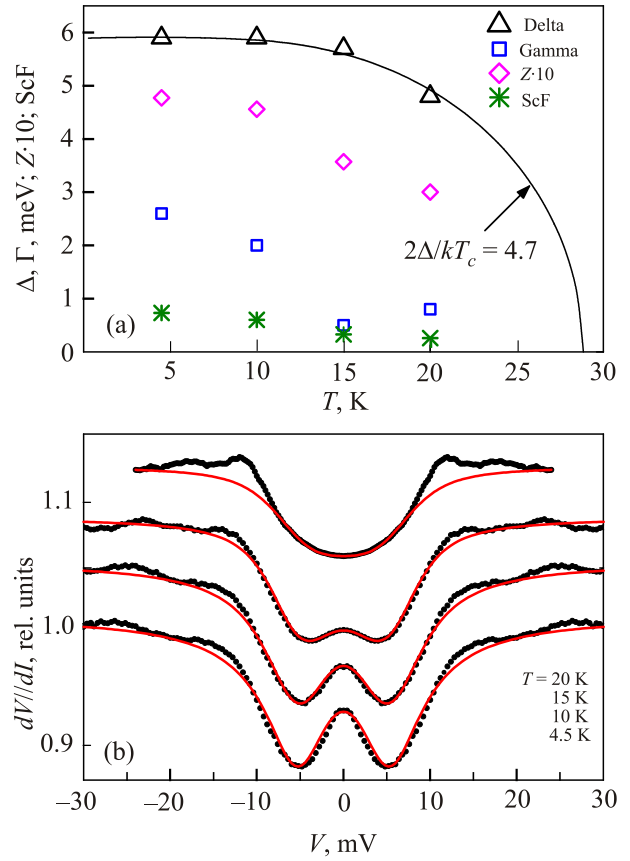

Fig. 8. (Color online). Temperature dependence of the SC gaps Δ, broadening parameters Γ, barrier strengths Z and scaling factor (ScF) (see Appendix in Ref. [23] to learn the meaning of these parameters) received from the BTK fit for the PC ($R \approx 75$ Ω) from Fig. 5. Solid line is BCS-like curve (a). Examples of the symmetrized experimental dV/dI (circles) and calculated ones (lines) within the BTK model [5] for several temperatures (b).

tween these two compounds is that for sample with $x = 0.25$ superconductivity coexist with spin-density wave order.

The obtained coupling strength values correspond well to those $2\Delta/k_B T_c = 2.5$–4 for another hole-doped system from this family $Ba_{0.55}K_{0.45}Fe_2As_2$ measured by the same PCAR technique in [12]. Besides, the lower value of $2\Delta/k_B T_c = 2.0$–2.6 is extracted for the similar system $Ba_{0.6}K_{0.4}Fe_2As_2$ by PC study in [13]. At the same time, the gap value obtained from ARPES measurements [15] for the compound with the highest T_c ($x = 0.4$) is maximal (around 10.5 meV) for the inner Γ barrel and minimal (around 3 meV) for the outer Γ barrel. However, as in the case of sample with $x = 0.25$, we could not resolve unequivocally the second gap features. Probably, due to short mean free path of electrons caused by strong elastic scattering we measure some averaged gap by PCs or, it is not excluded, merging of small and large gaps. Also scanning tunneling spectroscopy measurements [24] carried out on similar compound $Sr_{0.75}K_{0.25}Fe_2As_2$ resolved only one gap, which variates by 16% on a 3 nm length scale, with average $2\Delta/k_B T_c = 3.6$.

4. Conclusions

PC studies of Josephson effect and Andreev reflection were carried out on the iron-based superconductor $Ba_{1-x}Na_xFe_2As_2$ with $x = 0.35$ and 0.25. We succeed to detect and study the ac Josephson effect in PCs between $Ba_{1-x}Na_xFe_2As_2$ crystals and counterelectrodes from Pb, Ta, and Nb. Correspondence of the distance between Shapiro steps to the relation $2eV = \hbar\omega$ and observed critical current dependence on the microwave power (ScS with of Pb) support the presence of the s-wave singlet pairing symmetry in this new superconductor.

Analysis of the measured PC dV/dI spectra with Andreev-reflection features shows that at small biases the diffusive regime of the current flow realizes, whereas at the further bias increase the transition to the thermal regime in PCs occurs. In the latter case the shape of dV/dI is defined by the specific resistivity $\rho(T)$ of the investigated sample and the noticed asymmetry of the PC spectra is influenced by the thermopower $S(T)$ behavior. In the spectroscopic regime far below T_c it was possible to detect AR-like zero-bias minima in the range $\pm$ (5–15) mV. Applying of the BTK fit gives the reasonable values of $2\Delta/k_BT_c = 3.6 \pm 1$. The features on dV/dI which could be due to the manifestation of the second SC gap appeared very seldom and were not reproducible. This do not allow us to make a detailed numeric analysis of the second SC gap.

Acknowledgements

1. M. Rotter, M. Tegel, and D. Johrendt, *Phys. Rev. Lett.* **101**, 107006 (2008).

2. Kalyan Sasmal, Bing Lv, Bernd Lorenz, Arnold M. Guloy, Feng Chen, Yu-Yi Xue, and Ching-Wu Chu, *Phys. Rev. Lett.* **101**, 107007 (2008).

3. A.A. Kordyuk, *Fiz. Nizk. Temp.*, **38**, 1119 (2012) [*Low Temp. Phys.* **38**, 888 (2012)].

4. P. Seidel, *Supercond. Sci. Technol.* **24**, 043001 (2011).

5. D. Daghero, M. Tortello, G.A. Ummarino, and R.S. Gonnelli1, *Rep. Prog. Phys.* **74**, 124509 (2011).

6. I.O. Kulik and I.K. Yanson, *Josephson Effect in Superconducting Tunneling Structures*, John Wiley & Sons, Incorporated (1972).

7. A. Barone and G. Paterno, *Physics and Applications of the Josephson Effect,* New York: Wiley (1982).

8. Xiaohang Zhang, Yoon Seok Oh, Yong Liu, Liqin Yan, Kee Hoon Kim, Richard L. Greene, and Ichiro Takeuchin, *Phys. Rev. Lett.* **102**, 147002 (2009).

9. Xiaohang Zhang, Shanta R. Saha, Nicholas P. Butch, Kevin Kirshenbaum, Johnpierre Paglione, Richard L. Greene, Yong Liu, Liqin Yan, Yoon Seok Oh, Kee Hoon Kim, and Ichiro Takeuchi, *Appl. Phys. Lett.* **95**, 062510 (2009).

10. Takayoshi Katase, Yoshihiro Ishimaru, Akira Tsukamoto, Hidenori Hiramatsu, Toshio Kamiya, Keiichi Tanabe and Hideo Hosono, *Nat. Commun.* **2**, 409 (2011).

11. S. Döring, M. Monecke, S. Schmidt, F. Schmidl, V. Tympel, J. Engelmann, F. Kurth, K. Iida, S. Haindl, I. Mönch, B. Holzapfel, and P. Seidel, *J. Appl. Phys.* **115**, 083901 (2014).

12. P. Szabó, Z. Pribulová, G. Pristáš, S.L. Bud'ko, P.C. Canfield, and P. Samuely, *Phys. Rev. B* **79**, 012503 (2009).

13. Xin Lu, W.K. Park, H.Q. Yuan, G.F. Chen, G.L. Luo, N.L. Wang, A.S. Sefat, M.A. McGuire, R. Jin, B.C. Sales, D. Mandrus, J. Gillett, Suchitra E. Sebastian, and L.H. Greene, *Supercond. Sci. Technol.* **23**, 054009 (2010).

14. Yu.G. Naidyuk, O.E. Kvitnitskaya, I.K. Yanson, S. Aswartham, G. Fuchs, K. Nenkov, and S. Wurmehl, *Phys. Rev. B* **89**, 104512 (2014).

15. S. Aswartham, M. Abdel-Hafiez, D. Bombor, M. Kumar, A.U.B. Wolter, C. Hess, D.V. Evtushinsky,V.B. Zabolotnyy, A.A. Kordyuk, T.K. Kim, S.V. Borisenko, G. Behr, B. Büchner, and S. Wurmehl, *Phys. Rev. B* **85**, 224520 (2012).

16. K.K. Likharev, *Dynamics of Josephson Junctions and Circuits*, Philadelphia, PA: Gordon and Breach (1986).

17. O.P. Balkashin, I.I. Kulik, I.K. Yanson, Yu.G. Litvinenko, and V.T. Zagoskin, *Fiz. Nizk. Temp.* **16**, 321 (1990) [*Sov. J. Low Temp. Phys*, **16**, 176 (1990)].

18. Yu.G. Naidyuk and I.K. Yanson, *Point-Contact Spectroscopy*, Springer Series in Solid-State Sciences Springer Science+Business Media, Inc, vol. 145 (2005).

19. L. Wray, D. Qian, D. Hsieh, Y. Xia, L. Li, J.G. Checkelsky, A. Pasupathy, K.K. Gomes, C.V. Parker, A.V. Fedorov, G.F. Chen, J.L. Luo, A. Yazdani, N.P. Ong, N.L. Wang, and M.Z. Hasan, *Phys. Rev. B* **78**, 184508 (2008).

20. B.I. Verkin, I.K. Yanson, I.O. Kulik, O.I. Shklyarevski, A.A. Lysykh, and Yu.G. Naydyuk, *Solid State Commun.* **30**, 215 (1979).

21. I.O. Kulik, *Fiz. Nizk. Temp.* **18**, 440 (1992) [*Sov. J. Low Temp. Phys.* **18**, 302 (1992)].

22. Y.J. Yan, X.F. Wang, R.H. Liu, H. Chen, Y.L. Xie, J.J. Ying, and X.H. Chen, *Phys. Rev. B* **81**, 235107 (2010).

23. Yu.G. Naidyuk, O.E. Kvitnitskaya, L.V. Tiutrina, I.K. Yanson, G. Behr, G. Fuchs, S.-L. Drechsler, K. Nenkov, and L. Schultz, *Phys. Rev. B* **84**, 094516 (2011).

24. Can-Li Song, Yi Yin, Martin Zech, Tess Williams, Michael M. Yee, Gen-Fu Chen, Jian-Lin Luo, Nan-Lin Wang, E.W. Hudson, and Jennifer E. Hoffman, *Phys. Rev. B* **87**, 214519 (2013).